EXPERIMENTAL INVESTIGATION OF THE EFFECT OF GRILLE STRUCTURE TO THE OUTDOOR UNIT OF ROOM AIR CONDITIONER

Yadong WU[1], Jie TIAN[2], Hua OUYANG[2], Zhaohui DU[2]

1 School of Aeronautics and Astronautics Shanghai Jiao Tong University, Shanghai, China

2 School of Mechanical Engineering Shanghai Jiao Tong University, Shanghai, China

SUMMARY

Aerodynamic and noise performance parameters and flow fields near the exit of the outdoor unit of air conditioner with and without grilles are studied with a standard test rig and Particle Image Velocimetry (PIV). The grilles used in this study include two common grilles from the market and one newly-designed grille. The newly-designed grille is designed according to the detailed flow field of the outdoor unit and has an involute-curve shape. Experimental measurements are carried out to validate the effect of grille to the noise and the flow field of outdoor unit. The results indicate that the grille structure will affect the flow rate, the flow field, and the noise level of outdoor unit. The effect of the rectangle shape grille was greatest among three grilles, and the newly-designed grille with involute-curve shape is better, which make the flow uniform and reduce the noise level of the outdoor unit compared with two common grilles. And the methods that combine flow field and noise radiation presented in this research are useful to the designer to decide which grille will be chosen.

INTRODUCTION

There is a market demand for quieter outdoor unit of air conditioners. It is important to keep the noise generated by the fan system as low as possible while providing enough airflow. The fan and the outlet grille are subject to fluctuating forces resulted from the flow interaction with the different parts of the neighborhood compartment of the air conditioner. These fluctuations lower the aerodynamic efficiency and generate noise.

Until recently, the visualization of the flow field has relied mainly on experiments because the unsteady flow field in the turbomachine is not easy to calculate. Akaike et al. (1993) [1] investigated the behavior of the vortical flow inside and outside of propeller fan rotor using Laser Doppler Velocimetry (LDV). It showed that a vortical structure with reverse flow was observed just

upstream of the shroud at a low flow rate. Jang et al. (2001) [2, 3] also studied the vortical flow of propeller fan rotors of air conditioners using LDV measurements and Larger Eddy Simulation. It was found that three vortex structures were formed near the propeller fan rotor tip. The effects of the unsteady behavior of the vortex structure on pressure fluctuation in the rotor blade passage were also investigated. LDV is a point measurement technique, while PIV is a surface measurement technique. The former consumes a lot of time comparing with the latter. PIV is one of the most powerful tools to measure the flow field of turbomachinery. Jiang (2006, 2007) [4, 5] investigated the relationship between air flow field and aerodynamic noise of outdoor unit of air conditioner without a grille. Tip vortex patterns were measured by PIV technique. It was shown that the tip vortex was generated from the blade suction surface, and that high turbulence intensity would lead to increase aerodynamic noise. Estevadeordal et al. (2000) [6] investigated the characteristics of the flow in a low-speed axial fan using Digital Particle Image Velocimetry (DPIV). These measurements revealed steady and unsteady flow features at several operating points and allowed a composite DPIV image around the entire fan blade to be made. This composite image was compared with a panel code simulation, and the main differences found between them were attributed to local viscous effects such as flow separation and wake unsteadiness that were not included in the panel code implementation. Lee et al. (2003) [7] used PIV to measure an axial fan model of the outdoor cooling fan used for commercial air conditioners. The velocity fields in the radial and axial planes show clearly the periodic variations of flow structure and periodic shedding of the tip and trailing vortices at different fan blade phase according to phase-averaged technique. Yen et al. (2006) [8] used PIV to measure the exit flow field of a low-speed axial fan, which included the shrouded, shroudless, and winglet-blade types. The flow patterns on the radial and axial planes showed that a vortex always existed near the exit of the fans at various impeller angles. The above investigations can reveal the detailed flow field of rotor which has a simple structure.

The flow field of outdoor unit of air conditioner with grille is more complex than that of a single axial fan system. The outdoor unit includes heat exchanger, bellmouth, bracket of motor, and grille. The discharge flow of axial fan and its interaction with downstream grille should affect the aerodynamic performance of the outdoor unit and the overall sound pressure level. The broadband noise of room air conditioner with grilles has been investigated using experimental and numerical methods by Tian in 2009[9], where the noise characteristics of two types of grille have been discussed in detail. However, the detailed flow fields were not presented, and the relationship between noise and flow field was not discussed. In air conditioning industry, the designers do not care the shape of grille, and usually make a simple one. In the present study, a newly-designed grille was present according to the demands of market for low noise level, there were total three grilles investigated in this paper plus two ordinary grille used in the outdoor units. The noise level and internal flow field of an outdoor unit with three different grilles have been investigated experimentally. The relationship between the flow field and the noise radiation was revealed in this paper. Based on the aerodynamic and aeroacoustic results, the flow fields of the three cases with different grilles were compared, and the effect of the grille to the flow rate and noise level of the outdoor unit was evaluated. And the results showed that the newly-designed grille can reduce the noise level of outdoor unit.

EXPERIMENTAL SETUP

Research objects

A common commercial split-type room air conditioner outdoor unit is selected as the research object. As shown in Fig. 1, the outdoor unit consists of heat exchanger, motor supporting frame, motor, axial flow fan, bellmouth, and grille. The fan is a propeller-type one with three forward swept blades. The tip diameter of the fan rotor is 470 mm, and the hub/tip ratio is 0.34. The rotating speed of the rotor is 780 rpm at design condition. About 25 % of the tip chord of rotor is covered by

a 60 mm thickness bellmouth, and the clearance between the fan blade tip and the bellmouth is 8 mm.

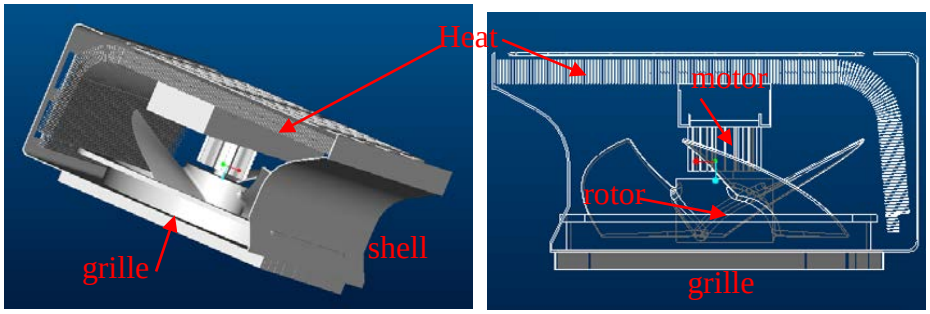

Fig. 1 Perspective view and top view of the outdoor unit of room air conditioner with grille

Two ordinary grilles, with denomination of Type-A, Type-B, are selected in this study, which were used by many manufacturers in the outdoor unit due to their simple structure. The Type-A grille is rectangular with a size of 540*540 mm. The shape of the horizontal struts, which have a rounded leading-edge and a blunt trailing-edge. The Type-B grille is circular with a maximum diameter of 500 mm. It is made up of 12 annular and 24 radial struts with circular cross sections. The interval of the radial struts is 15° in the circumferential direction. In order to make a quiet outdoor unit for air conditioner, the grille must be designed according to the flow field of outdoor unit. For that respect, a new grille is designed named Type-C grille. Type-C grille is more complicated. It has 32 involute-curve shape struts supported by several annular struts, as shown in Fig. 4. The involute-curve shape is obtained according to the characteristic of the trailing edge of the axial flow fan. The cross section of the involute-curve shape struts is circular arc, whose leading edge and trailing edge are also rounded. The involute-curve shape strut has a stagger angle corresponding with the stagger angle of the rotor blade, and the stagger angle varies in the spanwise. Through that, the outlet flow from the axial flow fan can be guided well across the grille with little loss and little shock. Furthermore, the involute curve is different from each other, that is to say, the distance divided by the annular struts is different, as shown in Fig. 4, the length of a, b, c and d is different. The aim is to reduce the noise level of axial flow fan and grille interaction. Then aerodynamic and aeroacoustic performance, and detailed flow will carried out to evaluate the three grilles.

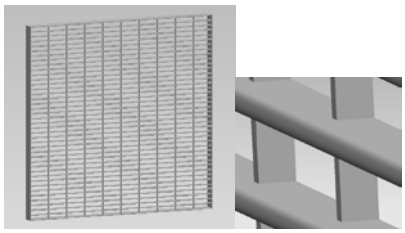

Fig. 2 Configuration of Type-A grille

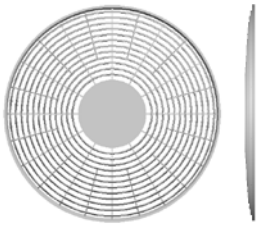

Fig. 3 Configuration of Type-B grille

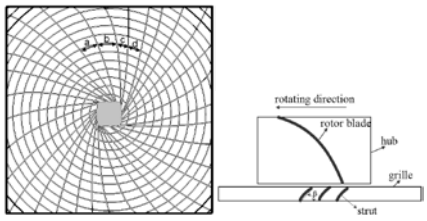

Fig. 4 Configuration of Type-C grille

Aerodynamic and Aeroacoustic experimental setup

The test rig of aerodynamic performance was built up according to the Chinese National Standard GB1236-2000 ‘Industrial fans: performance testing using standardized airways’[10], which is identical to ISO5801-1997, as shown in Fig. 5. The operation condition of the outdoor unit was at the fan design condition. Pressure was measured using a Pitot probe through precision differential pressure manometers. The value of P_{st} stood for the pressure rise of the outdoor unit, and through P_d, the flow rate would be obtained [10].

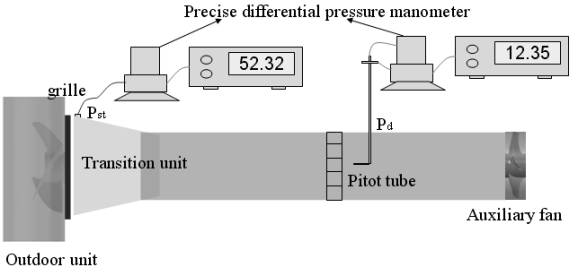

Fig. 5 Aerodynamic performance testing rig of outdoor units with grille

Noises from the outdoor unit included mechanical and electromagnetic noise from the electric motor and aeroacoustic noise. This paper mainly focused on the aeroacoustic noise. Noise measurements were carried out in a semi-anechoic chamber which had dimensions of 6*4.4*3.82 m. The A-weighted ambient noise level and the cut off frequency were 17 dBA and 165 Hz, respectively. The aeroacoustic test rig was set up according to ISO 3745.

PIV experiment setup

PIV is a multi-point instantaneous velocity field measurement instrument that provides quantitative velocity measurement and flow field visualization. The PIV measurement system consists of four parts: the PIV system, the traverse system, the particle-seeding device and the angular pulse trigger. A DANTEC PIV system has been adopted in the present experiment. It consists of two ND: YAG lasers, a high-resolution 8-bit Kodak Mega plus ES 1.0 digital camera, a dedicated PIV 2100 Processor, and software named Flow Manager. An Antari Z1500 Series atomization device is chosen as the particle-seeding device. It can generate 4.42 μm seeding particles that have excellent tracing characteristic to meet the demands. An ONO SOKKI FG-100 infrared trigger is adopted to excite the PIV measurement at decided blade phase locations. The corresponding PIV images are analyzed with a standard cross-correlation algorithm. In the present study an interrogation window of 32*32 pixels with a 25 % overlap is used. The pixel displacements are converted into equivalent spatial displacements by a transfer function. This transfer function is obtained by representing a photograph of a calibration image at the same location of the light sheet.

Three types of surfaces have been measured using PIV. The orientation and representative locations of these surfaces are shown in Fig. 6. Plane1-small planes are measured in order to capture the detailed flow downstream of the grille. Plane2 is carried out at different axial positions downstream of the grille. In order to check the effect of the blade phase to the grille, the meridian surfaces assigned as plane1-large and plane1-small are carried out at different blade azimuth, as shown in Fig. 7. Six blade azimuths covering the entire flow passage between the two blades are adopted and the interval angle is 20 degrees. In the present study the ensemble average number was set to 2000, so the unsteady instantaneous characteristics could be reduced at the most.

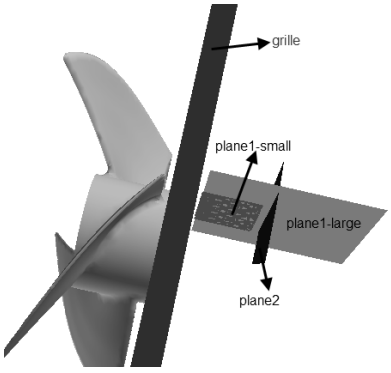

Fig. 6 PIV measuring surfaces at downstream of the grille

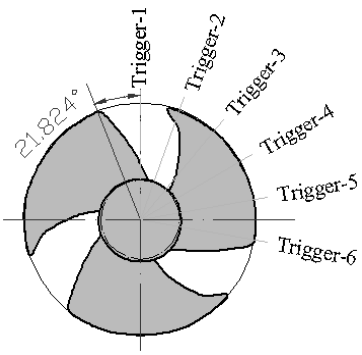

Fig. 7 Blade position at different triggers in PIV measurement

RESULTS AND DISCUSSION

Aerodynamic performance

Fig. 8 shows the normalized non-dimensional aerodynamic performance curve of the outdoor unit for the three grille cases. The non-dimensional volume flow rate coefficient φ and the non-dimensional rotor speed n_s are defined as follow,

$$\varphi = \frac{Q}{\pi r_{tip}^2 u_{tip}} \tag{1}$$

$$n_s = \frac{n}{n_{\max}} \tag{2}$$

where Q is the volume flow rate (m^3/s), r_{tip} the radius of the rotor (m), u_{tip} the rotating speed at the rotor tip (m/s), and n the rotating speed of the rotor (rpm), n_{max} the maximum rotating speed of the rotor (rpm).

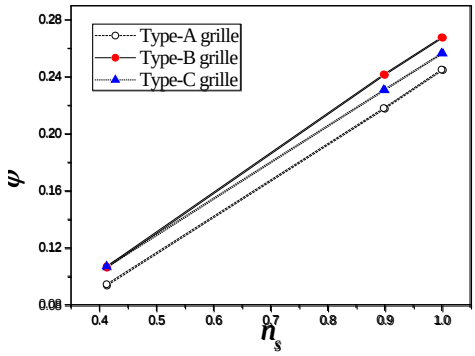

Fig. 8 Non-dimensional aerodynamic performance curves of the outdoor unit with grilles

At the same rotating speed, the non-dimensional flow rate is the highest for the Type-B grille case, and the difference between Type-C grille case is about 4.3%. At the low rotating speed, the flow rates for the Type-B and the Type-C grille cases are almost the same. The flow rate for the Type-A grille case is the lowest. It can be concluded that the potential pressure loss with the Type-A grille is larger than the other two cases.

Noise measurement results

The total SPL and 1/12 octave spectrums of outdoor unit with different grilles were measured at rotor rotating speed of 780 rpm, as shown in Fig. 9. The total SPL increases by 5.32 dBA, 3.95 dBA, and 2.75 dBA, respectively, with the three grilles, compared with 48.45 dBA(without grille). The SPL with Type-A grille is the largest, and the newly-designed Type-C grille can reduce noise level compared to the other two grilles. The noise spectrums in Fig. 9 indicate that the aerodynamic noise contains both broadband and discrete tonal noise. The latter is mainly generated from the unsteady aerodynamic force fluctuation of the rotor blades. The peak tone frequencies coincide with the blade passing frequency (BPF) and its harmonics. For Type-A grille, there is a highest noise level at low frequency 20 Hz. Then the noise level reduces fast until the frequency is reached to 145 Hz. At this time 4th harmonics appears and then the noise level reduces slowly with increase of frequency. The noise level of Type-A grille case is so high at low frequency that it covers the basic and 2nd harmonic of BPF contrast to the noise level without grille case. That is to say noise within this frequency range is mainly caused by Type-A grille. For Type-B and Type-C grille cases, it is found that the discrete tonal noise has a little increase at its harmonics of BPF, at basic BPF, Type-B grille reduce the noise level by 8 dB compared to without grille case.

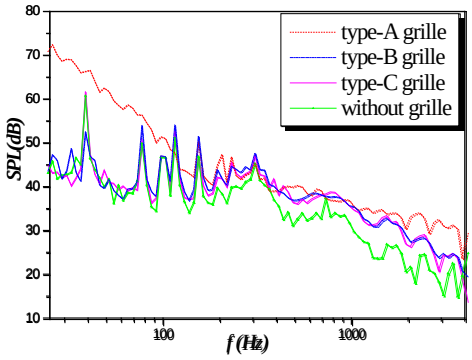

Fig. 9 1/12 octave spectrum of outdoor unit with different grilles

Flow field analyses

It is essential and instructive to choose particular sections for the visualization of flow patterns of outdoor unit with grille. For the case without grille, the tip vortexes, marked with ‘a’ and ‘b’, are clearly captured at the outlet of the fan, as shown in Fig. 10. Across the fan, the tip vortex flows off the blade suction surface. The vortex strength dissipates and encompasses a larger region. The vortex plays a major role in the flow field near the blade tip and has a large blockage effect to the flow. When a grille is fixed on, this phenomenon is changed. Fig. 11 shows the velocity vectors in the Plane1-large surface of different grilles at two different trigger. The tip vortex is scattered by the grille and no clear vortex is captured for Type-B and Type-C grille cases, while, the velocity in the tip region represent a little fluctuation. For Type-A grille case, there is still a vortex in the tip region at the outlet, marked as “c” and “d”, respectively, in Fig.11. The vortex core position changes with the change of the trigger position. Besides the vortex in the tip region, there is a newly-generated vortex near the hub of fan, marked as “e” and “f”, respectively, in Fig.11. The low speed flow near the hub of fan interaction with the struts generates the vortex, and the direction of this vortex is opposite to the one in the tip region. These vortexes block the flow from the outdoor unit, so the flow rate of Type-A grille case is smallest at the same speed compared to the other two cases.

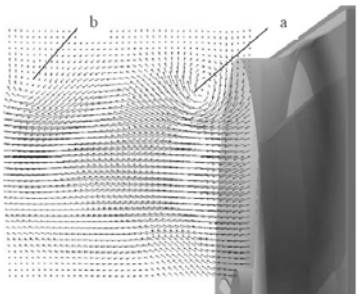

Fig. 10 Flow Field of outlet of outdoor unit without grille

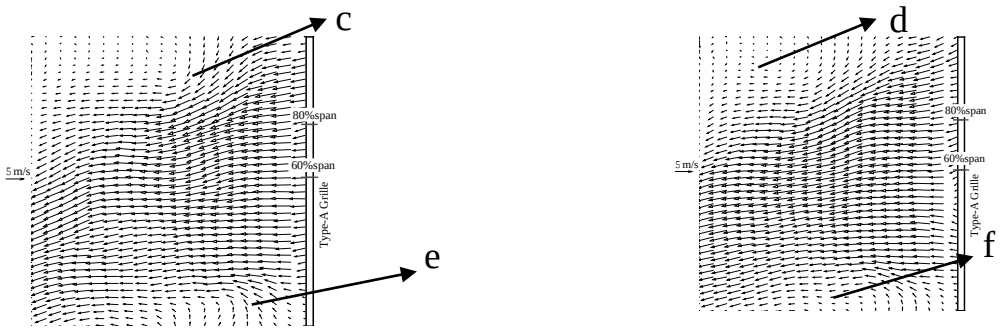

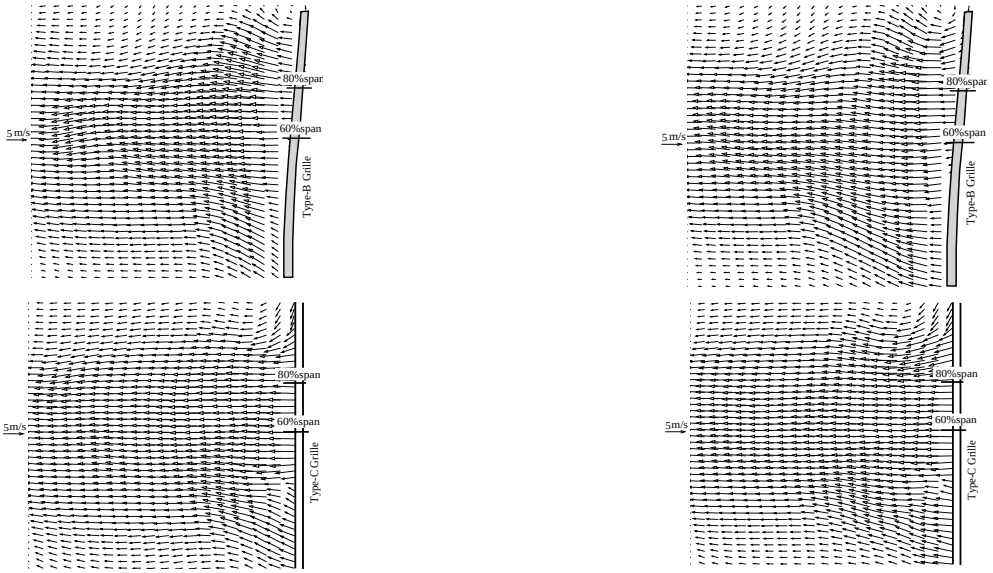

Fig. 11 Velocity vector at plane1-large outlet plane of outdoor unit with different types of grille at two trigger positions

Unitary averaged results are obtained by summing up the phase-locked ensemble averaged results at all 6 circumferential positions. The essential performance at the so-called steady condition can be obtained and the flow characteristics could be analyzed quantitatively. For the non-grille case, the flux rate is centered within the 60 %-80 % span, as shown in Fig. 12. The flow near the tip and hub focuses in the direction of 60 % span. Fig. 13 shows the unitary averaged results at the grille outlet, including velocity vector, the axial velocity magnitude contour and vorticity contour. The main flux rate domain is larger than that of the non-grille case. Especially for the Type-A grille case, the main flux rate focuses within 40 % to 85 % span, which is nearly half of the entire span. The velocity magnitude becomes small with grille, due to the resistance of the grille. While the flow focuses aslant and downward, different from the other two cases and the non-grille case, so the radial velocity component is larger than the other two cases, and the direction of radial velocity is opposite near the hub region. The flow pattern of Type-B grille case and Type-C grille case are almost the same, and the axial velocity is the main, which are close to the non-grille case. From the vorticity contour maps of three cases, there are two obvious vortexes at the outlet of Type-A grille case, and there is no vortex for Type-B and Type-C grille cases. The direction of the two vortexes is opposite, the magnitude is close, and the tip vortex core position is far from the outlet of the grille. The existence of two vortexes changes the flow direction of outlet of Type-A grille case. Through the unitary averaged results and the phase-locked ensemble averaged results, the Type-B and Type-C grille have little change to the outlet flow compared to the non-grille case, though the flow rate has a little reduction.

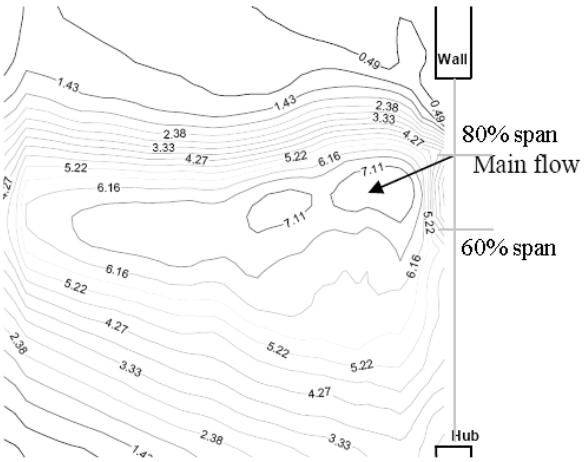

Fig. 12 Unitary averaged axial velocity contour map of non-grille case

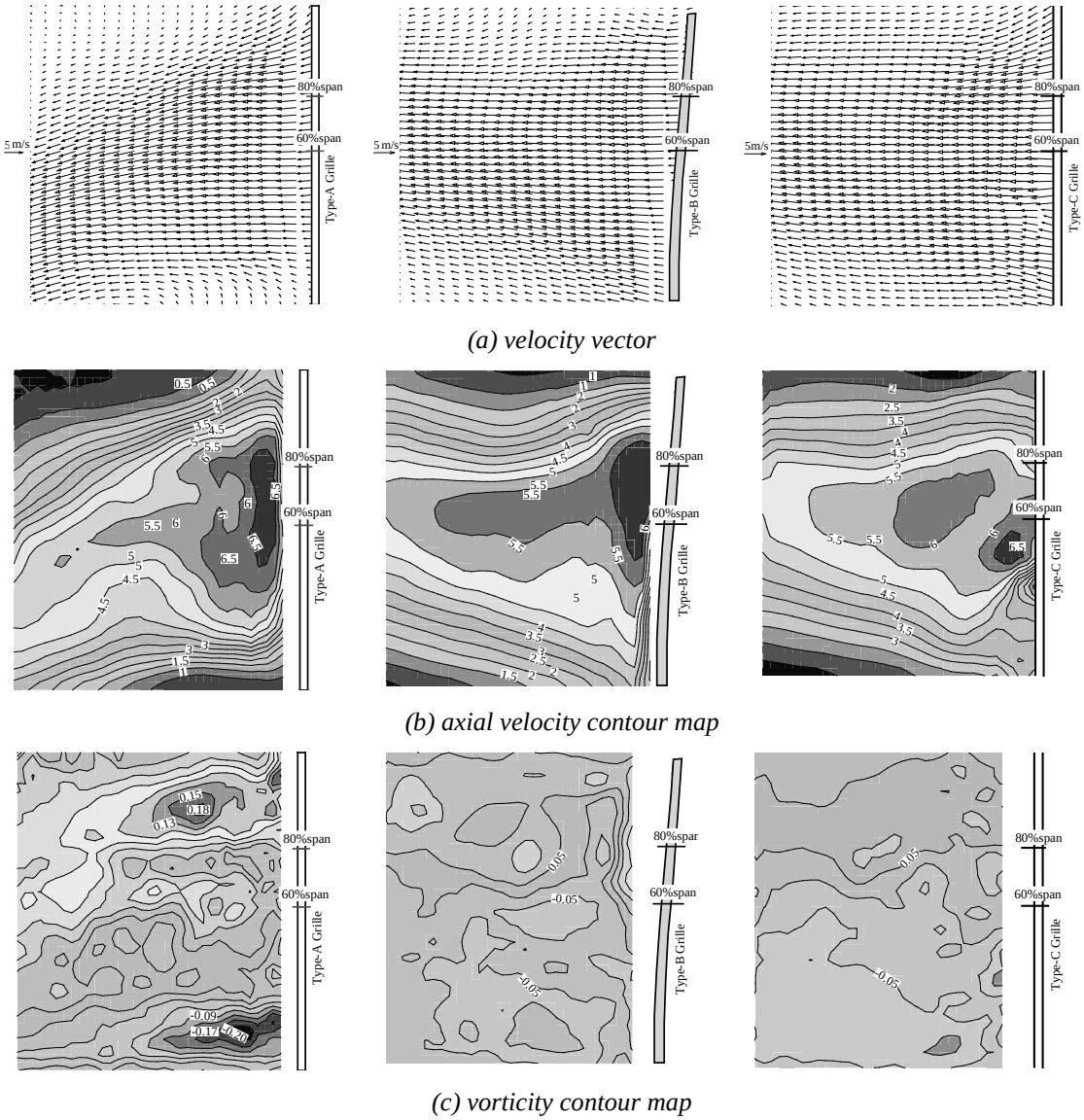

(a) velocity vector

(b) axial velocity contour map

(c) vorticity contour map

Fig. 13 Unitary averaged results of outdoor unit with three grilles at plane1-large

Fig. 14 shows the distribution of the axial velocity at three downstream axial positions, which have distances of 51.4 mm, 100.9 mm, and 150.3 mm, respectively, to the outlet of the grille. Near the grille outlet, the velocity distributions of three cases are close to each other, except at 0 to 20 % span. In that area, the velocity for the Type-A grille case is the smallest and that for the Type-B grille is the greatest. Further downstream, the flow patterns are different from each other. At 150.3 mm, the velocity magnitude for the Type-A grille case is smaller than the other two for most of the span. This means the dissipation of velocity for the Type-A grille case is quicker than the other two and the flow resistance is the largest among three grilles. For the Type-A grille case, the main flux rate area locates within 20 % to 50 % span and spreads in the hub direction. The flow patterns for the Type-B and the Type-C grille cases are close to each other. The magnitude for the Type-C grille case is larger than that for the Type-B grille case.

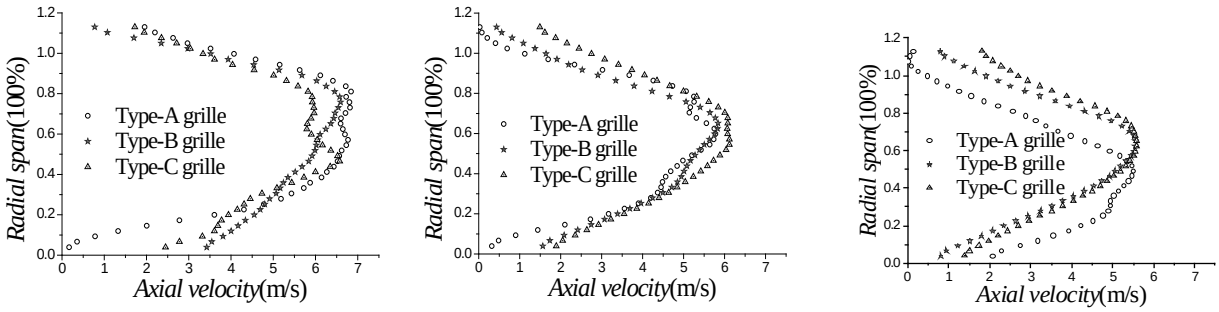

(a) 51.4 mm downstream of grille *(b) 100.9mm downstream of grille* *(c) 150.3mm downstream of grille*

Fig. 14 Axial velocity distribution at outlet plane1-large of three grilles from unitary averaged results

Fig. 15 shows the velocity vector and streamline map of outdoor unit without grille at plane2, where the radial velocity together with the tangential velocity can be captured. At the trailing edge from suction side to the pressure side, the directions of the flow velocity are changed apparently. At the flow field where vectors near blade trailing edge have been included, the radial velocity points from hub to shroud at blade suction side and from shroud to hub at blade pressure side. This changes how the generation process of blade trailing edge vortex. So, through the results, tip vortex and trailing edge vortex of rotor blade are clearly captured. Many velocity vectors are in the circumferential direction. While the grille is fixed on, the situation is changed. In Fig. 16, the velocity vectors of outdoor unit with three different types of grille are shown. Firstly, the tip vortex is captured in Type-A grille case at tip region, the streamline map can clearly show that. And there is no vortex in Type-B and Type-C grille cases, which mean the tip vortex of rotor blade is broken down, or large vortex in vertical direction is scattered completely into small length. Secondly, the trailing edge vortex of rotor blade is not captured in Type-B and Type-C grille cases, the annular struts of the two cases restructure the flow field of rotor blade wake. When grille is used behind rotor, the outlet flow of rotor interacts with the struts of grille, and the trailing edge wake is reduced by the annular struts with radial distribution, then the flow field downstream can be changed to uniform, and most velocity vectors are in circumferential direction. Compared to Type-B grille case, the outlet flow field of Type-C grille cases is more uniform. The involute-curve shape of the struts of Type-C grille is obtained according to the characteristic of the trailing edge of the axial flow fan, so they can eliminate the trailing edge vortex and make the flow uniform. While for Type-A grille case, the flow field in Plane2 is not uniform, the trailing edge vortex can be captured, too. And the trailing edge shape and intensity are changed because of the interaction with struts of Type-A grille.

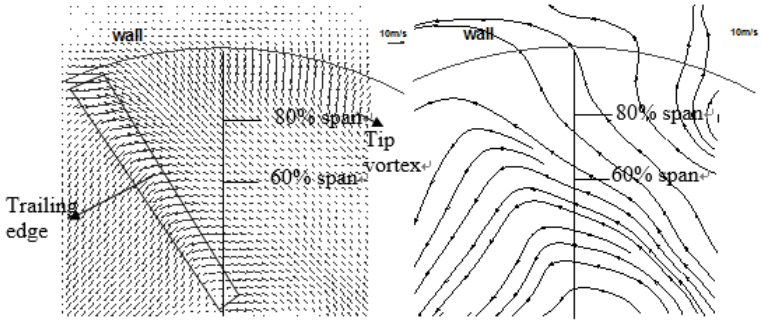

Fig. 15 Velocity at plane2 38 mm outdoor unit outlet without grille

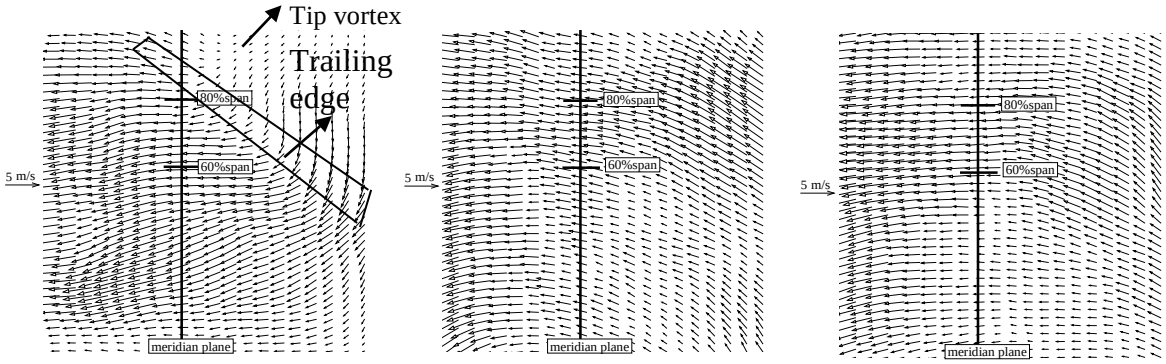

Type-A grille *Type-B grille* *Type-C grille*

(b) streamline maps

Fig. 16 Velocity at plane2 38 mm outdoor unit outlet with grilles

The detailed flow field near the grille on the Plane1-small surface at different triggers is shown in Fig. 17. Velocity defect can be clearly seen downstream of the horizontal struts of the grille. The unitary averaged velocity vector contour map obtained through six phase-locked ensemble results is shown in Fig. 18. There is obvious velocity defect behind the strut. The effect of the Type-A grille strut is more extensive than that of the other two grilles as shown in Fig. 19. At 40.8 mm axial position, the velocity defects behind the strut are obvious for all three grilles. At 70.0 mm, the strut wakes for the Type-B and the Type-C grille cases develop the same as the main flow. But for the Type-A grille case, the velocity fluctuates still.

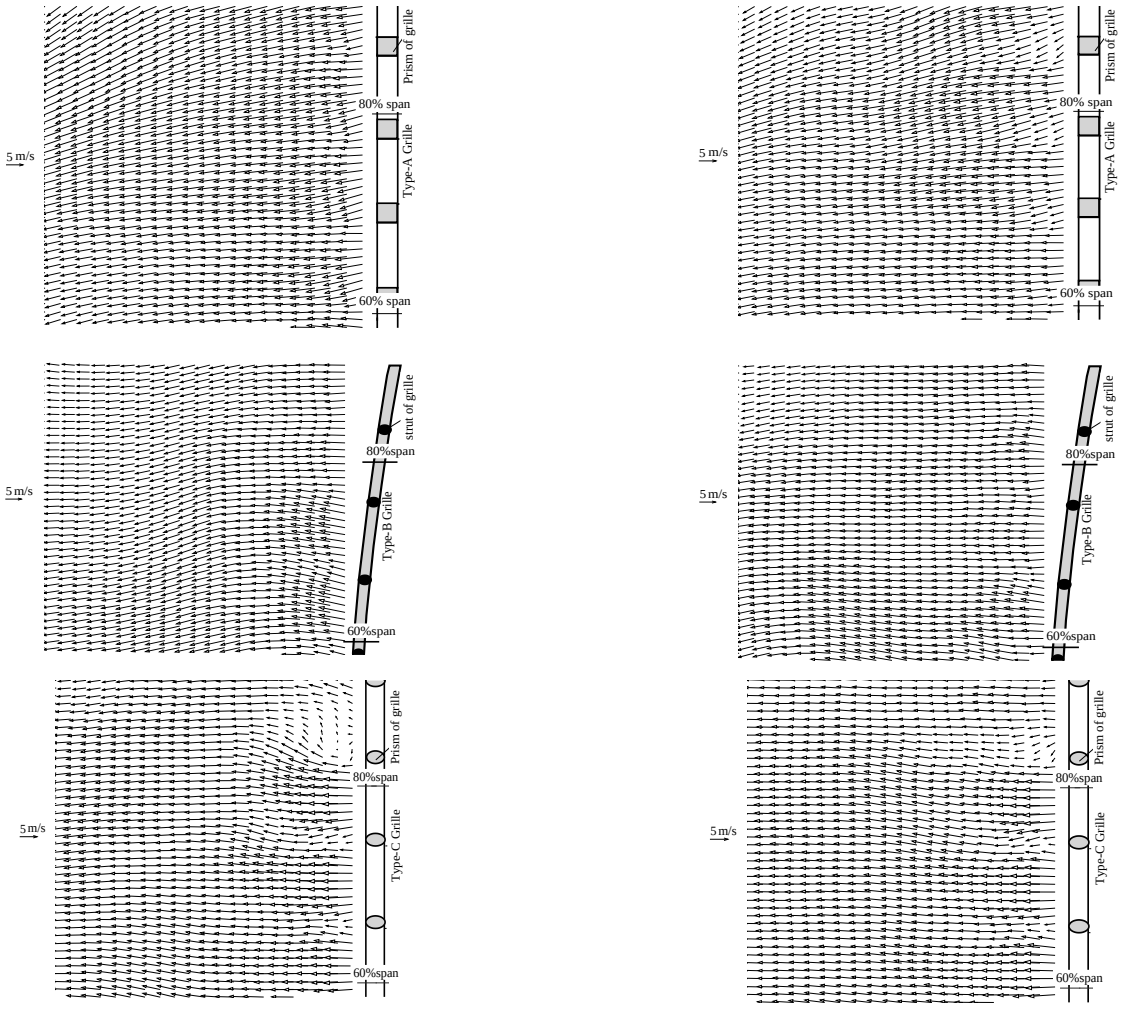

Fig. 17 Velocity vector at plane1-small outlet plane of outdoor unit with different types of grille at three trigger positions

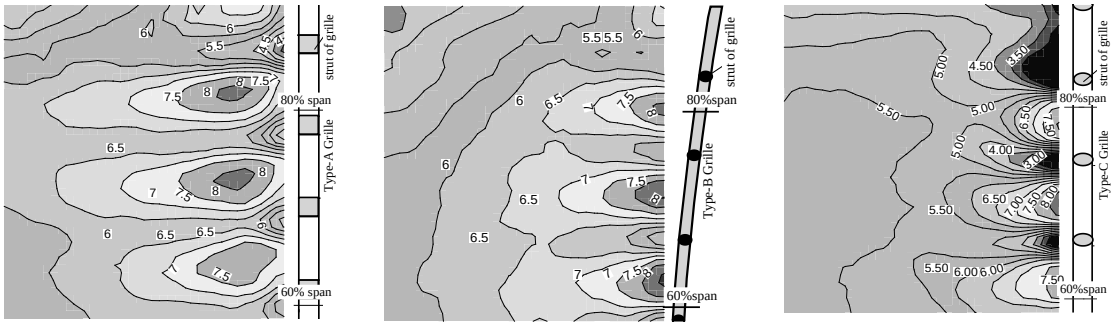

Fig. 18 Unitary averaged results of three grilles at plane1-small

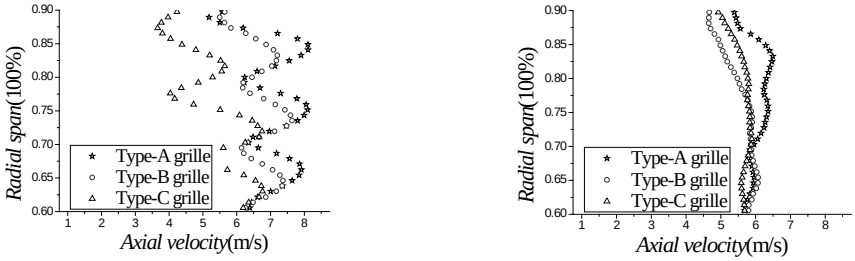

40.8 mm downstream of grille *70.0 mm downstream of grille*

Fig. 19 Axial velocity distribution at outlet plane1-small of three grilles from unitary averaged results

According to Powell's theory of vortex sound [12], sound is produced whenever vortex lines are stretched, dissipated and breakdown relative to aeroacoustic medium. The formulation of a region of vortex motion as an aeroacoustic source is a major step towards a physical understanding of aerodynamic noise. Vortex and the generation of the sound are closely related. Fig. 20 presents the unitary vorticity fields for the three grilles cases, where the strength and the spreading of the shedding vortex behind the strut are clearly represented. The vortex strength dissipation is the quickest for the Type-C grille case, while it is the slowest for the Type-A grille case. So it can be included that the noise level of Type-A grille case is the highest.

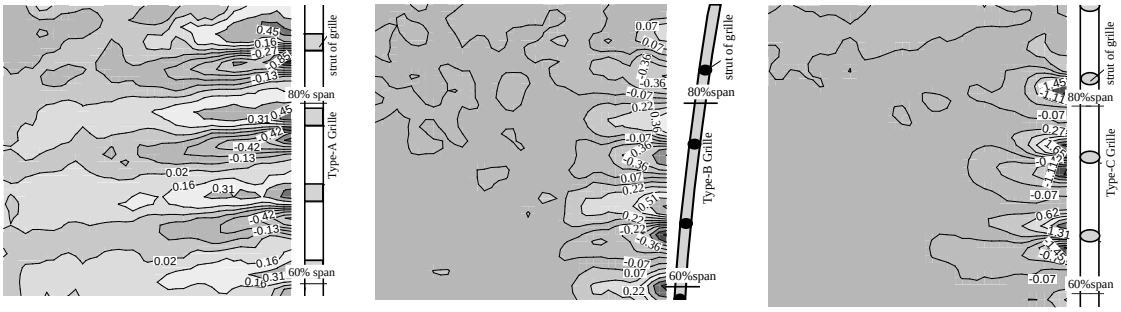

Type-A grille *Type-B grille* *Type-C grille*

Fig.20 Vorticity contour map of three grilles at plane1-small from unitary averaged results

CONCLUSIONS

The exit flow properties and performances of an outdoor unit with two common grilles from the market and a newly-designed grille are analyzed. The following conclusions are drawn from the results and discussions.

The newly-designed grille considers the flow of the axial flow fan in the outdoor unit, which can eliminate the effect of trailing edge vortex of axial flow fan and make the flow uniform. Furthermore, the involute-curve shapes are different from each other, which can reduce discrete

noise level. This type of grille has moderate pressure drag, so the outdoor unit has a middle flow rate compared to the other two grilles.

The square Type-A grille has a blockage effect to the outlet flow, as it can not eliminate the tip vortexes of the axial flow fan, meanwhile, there forms a vortex near the hub. And the Type-A grille enhance the strength of discrete noise and broadband noise level. Among the three grilles, it can increase the total noise level to 5.32 dBA, and the level is the largest.

For the round Type-B grille, it has the best air flow rate for the outdoor unit, and the difference between Type-C newly-designed grille case is about 4.3%. Meanwhile it enhances the broadband noise level, and form more wake deficit from the struts of the grille than that of newly-designed grille case. Based on the PIV results, the wake depth and the wake width of the Type-A grille and Type-B grille struts are stronger than that of newly-designed grille.

The present work is useful for the next phase of the research work, where both the aerodynamic and the noise performance of the outdoor unit will be further analyzed with the goal of designing excellent grille and providing CFD validation database.

REFERENCE

[1] S.Akaike, K. Kikuyama, – *Noise reduction of pressure type fans for automobile air conditioners,*ASME J. Vibr. Acoust., 115: 216-220. **1993.**

[2] C.M. Jang, M. Furukawa, et al. – *Analysis of vortical flow field in a propeller fan by LDV measurements and LES-Part I: three-dimensional vortical flow structures,* J. Fluids Eng. 123(4): 748-754. **2001.**

[3] C.M. Jang, M. Furukawa, et al. – *Analysis of vortical flow field in a propeller fan by LDV measurements and LES-Part II: unsteady nature of vortical flow structures due to tip vortex breakdown,* J. Fluids Eng. 123(4):755-761. **2001.**

[4] C.L. Jiang, J.P. Chen, Z.J.Chen, et al. – *Experimental and numerical study on aeroacoustic sound of axial flow fan in room air conditioner*, Applied Acoustics, 68:458-472. **2007.**

[5] C.L. Jiang, J. Tian, H. Ouyang, et al. – *Investigation of air-flow fields and aeroacoustic noise in outdoor unit for split-type air conditioner,* Noise Control Eng. J., 54(3):146-156. **2006.**

[6] J. Estevadeordal, S. Gogineni, W. Copenhaver, et al. – *Flow field in a low-speed axial fan: a DPIV investigation*, Exp Therm Fluid Sci, 23:11-21. **2000.**

[7] Lee, Sang-Joon, Choi, Jayho and Yoon, Jong-Hwan – *Phase-Averaged Velocity Field Measurements of Flow Around an Isolated Axial-Fan Model,* J. Fluids Eng. 125(6):1067-1072. **2003.**

[8] S. C. Yen, Lin, K. T. Frank– *Exit Flow Field and Performance of Axial Flow Fans*, J. Fluids Eng. 128(2):332-340,**2006.**

[9] J. Tian, H. Ouyang, and Y. D. Wu – *Experimental and numerical study on aerodynamic noise of outdoor unit of room air conditioner with different grilles*, International J. of refrigeration, 32(5):1112-1122. **2009.**

[10] GB1236-2000. Industrial fans: performance testing using standardized airways, Chinese National Standard, **2000.**

[11] FlowMap PIV Installation & User's guide, Dantec Measurement Technology, Denmark. **2004**

[12] A. Powell – *Theory of vortex sound,* J. Acoust. Soc. Am. 36:177-195. **1964.**